




Article

The Role of Calcite Dissolution and Halite Thermal Expansion as Secondary Salt Weathering Mechanisms of Calcite-Bearing Rocks in Marine Environments

Javier Martínez-Martínez ^{1,*} , Anna Arizzi ²  and David Benavente ³ 

¹ Spanish Geological Survey—Higher Council for Scientific Research (IGME-CSIC), 28003 Madrid, Spain
² Department of Mineralogy and Petrology, University of Granada, 18002 Granada, Spain; arizzina@ugr.es
³ Department of Earth Sciences and the Environment, University of Alicante, 03080 Alicante, Spain; david.benavente@ua.es
* Correspondence: javier.martinez@igme.es

Abstract: This research focuses on the analysis of the influence of two secondary salt weathering processes on the durability of rocks exposed to marine environments: chemical dissolution of rock forming minerals and differential thermal expansion between halite and the hosting rock. These processes are scarcely treated in research compared to salt crystallisation. The methodology followed in this paper includes both in situ rock weathering monitoring and laboratory simulations. Four different calcite-bearing rocks (a marble, a microcrystalline limestone and two different calcarenites) were exposed during a year to a marine semiarid environment. Exposed samples show grain detachment, crystal edge corrosion, halite efflorescences and microfissuring. Crystal edge corrosion was also observed after the laboratory simulation during a brine immersion test. Calcite chemical dissolution causes a negligible porosity increase in all the studied rocks, but a significant modification of their pore size distribution. Laboratory simulations also demonstrate the deterioration of salt-saturated rocks during thermal cycles in climatic cabinet. Sharp differences between the linear thermal expansion of both a pure halite crystal and the different studied rocks justify the registered weight loss during the thermal cycles. The feedback between the chemical dissolution and differential thermal expansion, and the salt crystallisation of halite, contribute actively to the rock decay in marine environments.

Keywords: halite; marble; limestone; linear thermal expansion coefficient; climatic cabinet



Citation: Martínez-Martínez, J.; Arizzi, A.; Benavente, D. The Role of Calcite Dissolution and Halite Thermal Expansion as Secondary Salt Weathering Mechanisms of Calcite-Bearing Rocks in Marine Environments. *Minerals* **2021**, *11*, 911. <https://doi.org/10.3390/min11080911>

Academic Editor: Alexander R. Cruden

Received: 13 July 2021

Accepted: 18 August 2021

Published: 23 August 2021

Publisher's Note: MDPI stays neutral with regard to jurisdictional claims in published maps and institutional affiliations.



Copyright: © 2021 by the authors. Licensee MDPI, Basel, Switzerland. This article is an open access article distributed under the terms and conditions of the Creative Commons Attribution (CC BY) license (<https://creativecommons.org/licenses/by/4.0/>).

1. Introduction

Rock weathering by salt crystallization is considered one of the most important processes acting on the building stones in monuments under marine environments [1–4]. In these cases, halite (NaCl) is the most frequent, if not the only, mineral phase observed in efflorescences and subefflorescences [4,5]. The presence of this salt in monuments is explained by means of different mechanisms for marine salt supply including capillary uptake, saline rainwater incursion, condensation of atmospheric humidity, or dry deposition of marine aerosol [2,4,6].

Halite can crystallise only when the environmental relative humidity is lower than its critical deliquescence point (75.3%) [7]. This reference value is nearly independent of temperature, and the influence of other salt species is slight. In dry environments (relative humidity lower than 75.3%), sodium chloride precipitates generating salt crystallization stresses on the solid structure of the rock that can cause the failure of the weakest parts of the rock. However, some studies conclude that halite is relatively ineffective generating crystallization pressures and, consequently, it generates a low level of physical damage in the built heritage [8–10]. Notwithstanding, several authors consider that halite damage is linked to other secondary weathering mechanisms such as thermal expansion [11] and/or

the dissolution of the host rock, mainly in the calcite fraction [12,13]. Nevertheless, these other two decay processes have received much less attention than the salt crystallization effect, despite the fact that the effectivity of the last one is thrown into question.

Calcite-bearing rocks (limestones and marbles) are widely used as building materials in both modern buildings and monuments, and their use is ubiquitous in façade claddings, pavements, interior and exterior structures, etc. The huge interest in the use of these rocks as building materials is justified mainly by their aesthetical properties and its good workability. However, in outdoor environments, they can undergo significant physical weathering especially when the presence of salty solutions in the porous system of the rock is high. Due to this fact, special attention must be paid to all the weathering processes acting on these building rocks in order to obtain a better understanding of the suitability of given dimension stone for certain applications. New advances in this topic contribute to achieving a more comprehensive knowledge of the rock decay risk, as well as to offering a higher guarantee of durability.

The aim of this paper is to analyse the effectivity of the thermal expansion and the chemical dissolution as secondary weathering mechanisms acting on the NaCl-CaCO₃ system. This study includes both in situ monitoring and laboratory simulations. On the one hand, the textural evolution of calcite-based rock samples (limestones, marbles and calcarenites) was analysed after one year of direct exposure under marine conditions. On the other hand, several tests were carried out in the laboratory in order to quantify the response of studied rocks during both thermal shock and chemical dissolution tests. Results will contribute to understand the real effects of the NaCl brine in the porous system of rocks and their consequences on the decay and conservation of the built heritage in marine environments.

2. Materials

Four different types of calcite-based rocks were selected for this study: a marble, a massive (low-porous) limestone, and two different types of calcarenite (Figure 1). Selection criteria attends to differences in porosity and pore-size distribution. Hand sample description was completed with microscope observations of thin sections under petrographic optical microscope (Axioskop 20, Zeiss, Oberkochen, Germany). Mineralogical composition of studied rocks was analysed by powder X-ray diffraction in a Philips PW-1710/00 (Philips, Amsterdam, Netherlands) diffractometer (Cu Ka radiation with a Ni filter and a setting of 40 kV and 40 mA). Rock porous system was characterised by means an Autopore IV 9500 (Micromeritics, Norcross, Georgia) mercury porosimeter.

Marble sample (Mb) correspond to a homogeneous white calcite marble. Rock texture is homeoblastic and xenoblastic, and the mean crystal size is about 740 µm, although crystal sizes of up to 2 mm have been observed. Mineralogically, it is constituted fundamentally of calcite (~99%) and very low quantities (2–5%) of other minerals such as quartz, muscovite, plagioclase, pyrite, apatite, and zircon. Porosity is lower than 1%.

The grey massive limestones (Ls) constitute a dense microcrystalline rock (crystal size of 20–40 µm) with porosity values ranging between 0.5 and 1.5%. Mineralogical composition corresponds to 98% of calcite and low quantities of clay and dolomite. The porous system is mainly centred on small pores (mainly fissures of ~2 µm in size) poorly connected.

The two calcarenites show marked textural differences. One of them (Cg) corresponds to a coarse-grained calcarenite (also named calcirrudite as the average grain size higher than 2 mm) with a high content of algal rhodolith (several centimetres in size), and, subordinately, bryozoans and foraminifera. Lithoclast content is very low (mainly quartz). The second calcarenite type (Cf) constitutes a fine-grained sandy calcarenite. Bioclast are mainly foraminifera and, subordinately, fragments of bryozoa, red algae and echinoderms. Lithoclasts (tens of microns in size) are mainly composed of rock fragments of both volcanic rocks and limestones, but some quartz grains can also be observed. Both selected varieties have a complex porous media characterised by high porosity (16.15–24.13%). In both

cases, porous system presents a main pore population centered in a narrow pore size range (0.2–1 μm for Cf and 0.08–1 μm for Cg).

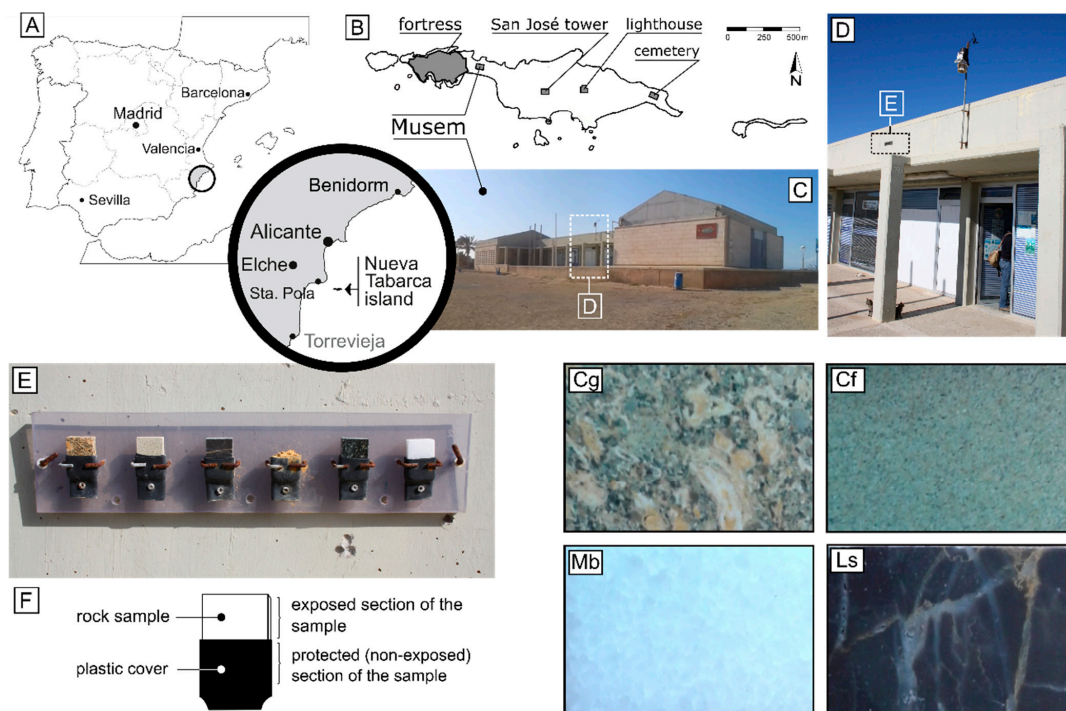


Figure 1. Geographical location of the Nueva Tabarca island (A,B). Location and position of the rock samples exposed to the marine environment (C–E) and sketch of the preparation of the samples (F). Studied lithotypes: coarse-grained calcarenite (Cg); fine-grained calcarenite (Cf); white marble (Mb) and grey massive limestone (Ls).

3. Methodology

The methodology followed in this study included both in situ monitoring and laboratory simulations.

3.1. In Situ Rock Weathering Monitoring

One sample of each lithology was exposed to a marine environment over the course of one year. Samples were located at the south façade of the museum building of the Nueva Tabarca Island (Figure 1). The museum location is in a completely flat plain and very close to the seacoast (50 m). Due to the absence of sheltering structures, all the samples present seaward exposure.

The exposed face of each rock was previously polished, and the lower half of the sample was covered with a heat shrink-wrap in order to protect it from weathering agents (Figure 1F). Before sample location in the Nueva Tabarca museum, rock surface was observed under a Scanning Electron Microscope in backscattering electron mode (BSE-SEM, S3000N, Hitachi, Tokyo, Japan). The microscope used in this study was a HITACHI S-3000 N (Hitachi, Tokyo, Japan) variable pressure SEM working at low vacuum. An Energy Dispersion Spectrometer (Bruker-XFlash 3001 EDS, Bruker, Billerica, MA, USA) is attached for chemical microanalysis and compositional mappings. SEM observations of rocks were carried out again after a one-year exposure to marine conditions. The same areas of the rock surface were used as checkpoints in order to compare the rock texture before and after the one-year exposure. Non-exposed (covered) parts of the samples were also analysed in order to corroborate that observed changes were directly related to marine exposure.

Local climatic parameters were measured during the exposure period by means of a weather station (Davis-Wireless Vantage PRO2, Davis Instruments Corp. Inc., Hayward,

CA, USA) which included a tipping-bucket rain gauge (Davis 7852) for rainfall measurements and a 12-bit smart Sensor (Davis 7315) to measure the relative humidity and air temperature with an accuracy of ± 0.5 °C above -7 °C, and $\pm 2\%$ from 10% to 100% relative humidity. The Data Acquisition System consisted of a WeatherLink (#6510USB) data logger.

3.2. Laboratory Simulation: Differential Thermal Expansion

The linear thermal expansion coefficient (α_T) of the studied rocks was determined by means of Thermomechanical Analysis (TMA). The equipment used is a Q400 TA Instruments Thermomechanical Analyser (Research Support Services, Alicante University, Alicante, Spain) that may work from -70 °C to 800 °C with a maximum strength of 2N. The linear thermal expansion of a pure crystal of halite was also measured. All samples were exposed to three heating–cooling cycles, ranging temperatures between 30 °C and 70 °C. Linear thermal expansion coefficient was calculated from the formula:

$$\alpha_T = \frac{1}{l_{0,T}} \cdot \frac{dl}{dT} \quad (1)$$

where $l_{0,T}$ is the length at a reference temperature.

Differential thermal expansion between halite crystals and the hosting rock was visually checked using an Environmental Scanning Electron Microscope (ESEM) (Centre for Scientific Instrumentation, Granada University, Granada, Spain). This microscope is a low-vacuum SEM with the ability to examine samples under a range of different environments. The environmental chamber can be manipulated in terms of atmosphere, temperature (-5 °C to 60 °C), and pressure (0 to 20 Torr). A rock sample previously filled with both halite efflorescences and subefflorescences was tested in ESEM with variable temperature conditions (from 3 to 50 °C) in order to observe differences in thermal expansivity.

Rock damages caused by differential thermal expansion between both halite crystals present in the porous system of rocks and the rock hosting were simulated in a climatic cabinet. The experiments used three prismatic samples (3 cm \times 3 cm \times 6 cm) of the studied rocks. Stone blocks were dried in an oven until a constant weight. Once dried, the blocks were immersed in a saturated NaCl solution for 10 h and then they were dried under room conditions for 14 h. The saturation-drying cycle was repeated 10 times in order to obtain both dense halite efflorescences and subefflorescences over and inside the samples.

The cabinet used for differential thermal expansion tests was a Sanyo-FE 300H/MP/R20 (Sanyo, Santa Fe Springs, California, USA) (inner volume: $675 \times 630 \times 650$ mm³), available at the University of Oxford, with a steady thermostat and an external temperature–moisture programmer. The cabinet was programmed with a 24-h temperature cycle. The air temperature during the cycle oscillated between 20 and 70 °C with an initial 7 h constant-speed heating ramp and 9 h of constant-speed cooling. Each cycle finished with 8 h at a constant temperature (20 °C). The relative humidity within the cabinets varied between 60% (at 20 °C) and 50% (at 70 °C). These values were selected to avoid any damage caused by halite crystallization in the porous system of rocks during the test. It was avoided by establishing the relative humidity inside the climatic cabinet under 75.3%. This value corresponds to the critical deliquescence point for halite. Consequently, dry conditions (RH < 75.3%) during the whole test guarantee the presence of halite inside the rock in its solid phase.

To remove the salts from the samples, they have been immersed in distilled water at 50 °C to prevent damage during cleaning, and the water was changed every day. Electrical conductivity of the water used to wash the samples was monitored to follow its degree of saturation, since the concentration of NaCl in the solution has a significant influence on it. Samples were considered clean when the electrical conductivity was stable around 0.3 mS/m while deionised water had a conductivity of 0.1 mS/m.

Changes in the appearance of samples were controlled visually during the experiment and their weight loss was recorded at the end of the experiment.

3.3. Laboratory Simulation: Chemical Dissolution

The chemical dissolution experiment was carried out in a saline solution, which represents the salt chemical weathering of studied rocks in saline environments. The experiment used 2 cm cubes of each lithology. Calcite dissolution was carried out in a stirrer cell, filled with a saline NaCl solution (pH of 8.44) at 25 °C and a constant atmospheric CO₂ concentration of 440 ppm. Under this experimental condition, only the calcite dissolution is produced and no other salts precipitate on the calcite surface. During the experiment, the solution was magnetically stirred at 300 rpm to ensure homogeneity. Dissolution conditions were maintained for 72 h. This test duration was established taking into account that, although the first isolated dissolution pits appear almost immediately (within the first 10 min of reaction) [14], the depth of these first pits is mainly around 0.3–0.6 nm and even after several hours of dissolution, some areas of the surface show only isolated shallow pits (~1 nm deep).

Two adjacent rock blocks (1.5 cm cubes) were obtained from each lithology. One of them was used for characterizing the porous system of the rock in fresh conditions. Pore size distribution was obtained in an Autopore IV 9500 (Micromeritics, Norcross, Georgia) mercury porosimeter. Pore size interval characterization by mercury intrusion porosimetry ranges from 0.006 to 200 µm. The other cube was used for the chemical dissolution experiment. After the test, the appearance of the weathered rock surface was observed under BSE-SEM. Moreover, pore size distribution of the weathered sample was measured by MIP.

4. Results and Discussion

4.1. Rock Textural Changes after Direct Exposure to Marine Environment

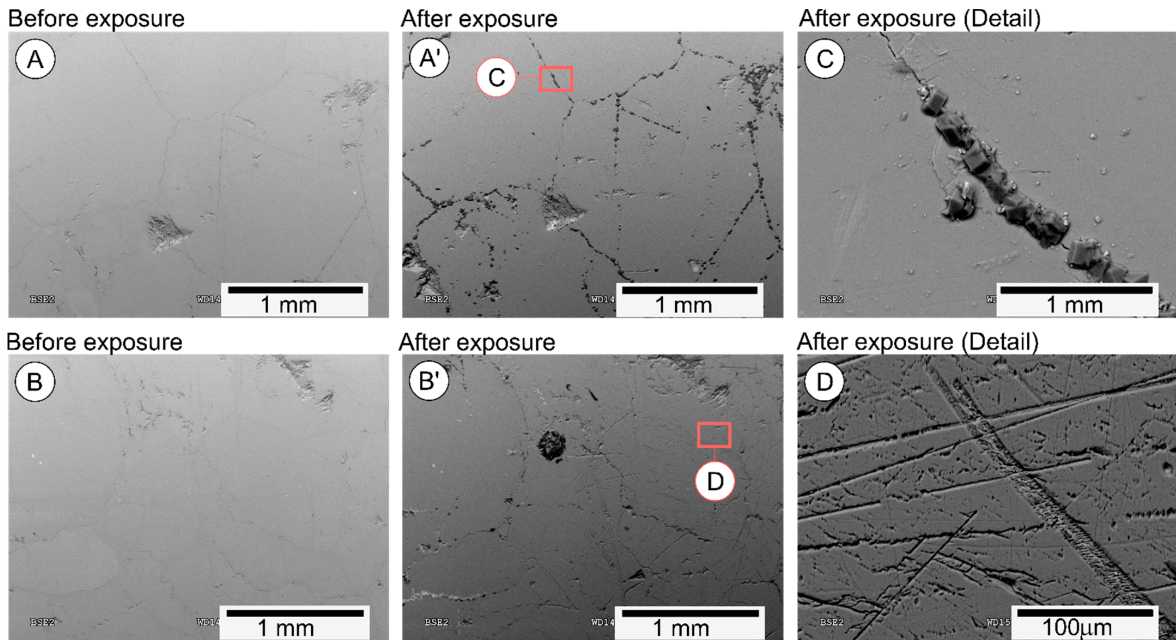
Rock samples were exposed to a Mediterranean semiarid climate (“Csa” according to Köppen–Geiger climate classification). Table 1 shows the climatic parameters measured in the Nueva Tabarca weather station. The region is characterised by hot, dry summers and mild, wet winters. The relative humidity is high due to the proximity of the sea, with an average annual value of 74.3%. Annual rainfalls are low (251 mm during the studied period) in accordance with the prevailing semiarid climate. During the summer, there are long periods of drought, with only short and punctual rainfalls. Torrential rains are characteristic in autumn and winter, reaching records of 66.6 mm in less than 12 h.

Table 1. Climatic data of Nueva Tabarca Island.

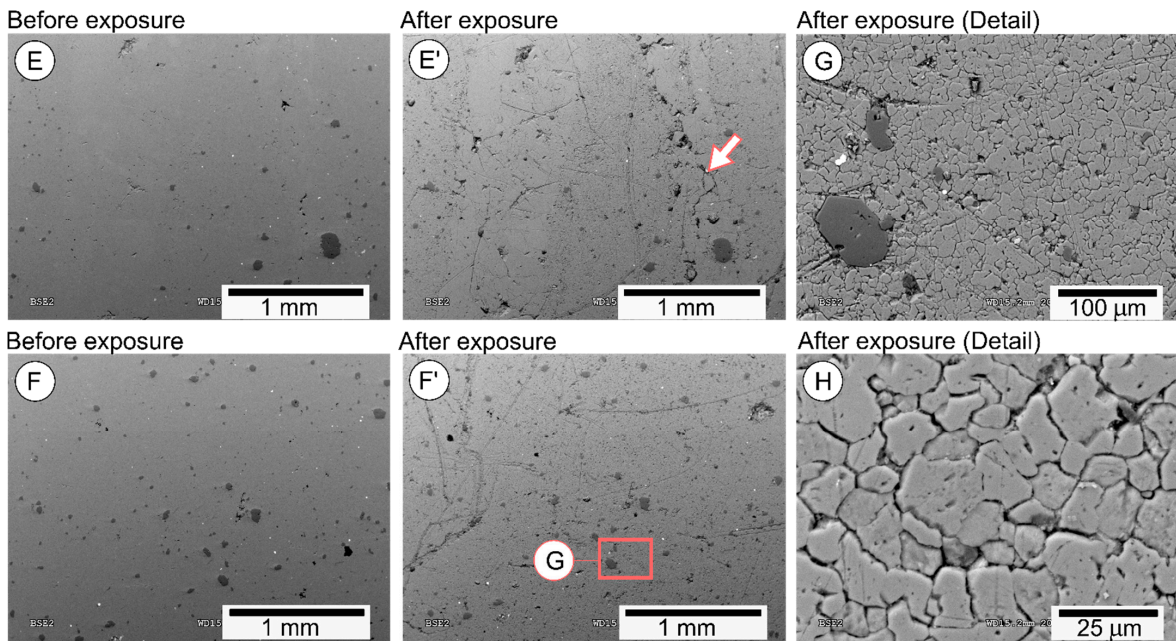
Month	Temperature (°C)			RH (%)			Rainfall (mm)
	Mean	Min	Max	Mean	Min	Max	
January	12.5	4.3	20.2	78.0	36.0	96.8	45.8
February	12.6	5.5	21.1	74.9	32.1	94.8	67.5
March	13.0	6.0	21.1	78.9	34.7	97.3	74.6
April	16.9	13.2	21.2	74.0	37.5	94.4	0.0
May	19.3	13.7	23.2	81.9	41.2	95.6	3.2
Jun	23.2	18.3	29.8	80.1	36.2	94.1	0.0
July	26.1	22.8	31.6	81.9	48.3	93.8	0.2
August	26.8	23.4	30.2	78.3	50.0	90.1	4.2
September	25.0	22.2	31.1	71.5	38.4	86.5	0.0
October	21.0	16.8	24.9	72.9	38.3	92.7	4.6
November	17.9	10.3	26.6	70.5	32.5	92.1	18.2
December	12.3	3.6	19.3	75.0	34.6	94.2	11.0

At the mesoscale, weathered samples do not show any noticeable decay sign with naked eye. Exceptionally, the shine of the polished surface of porous samples (it means, in Cf and Cg rock blocks) has been lost at some points due to the increase in roughness associated with weathering processes. This roughness increase also causes a colour change [15], especially visible in the dark rocks (Ls variety).

However, microscopically, there are significant textural changes in all the tested rocks. Figure 2A–D illustrates the textural evolution of studied rocks after direct exposure to the marine environment. Images show exactly the same area before and after the in situ test. Remarkable differences are observed between fresh and weathered surfaces, depending the developed decay patterns on the studied lithology.



(A)



(B)

Figure 2. Cont.

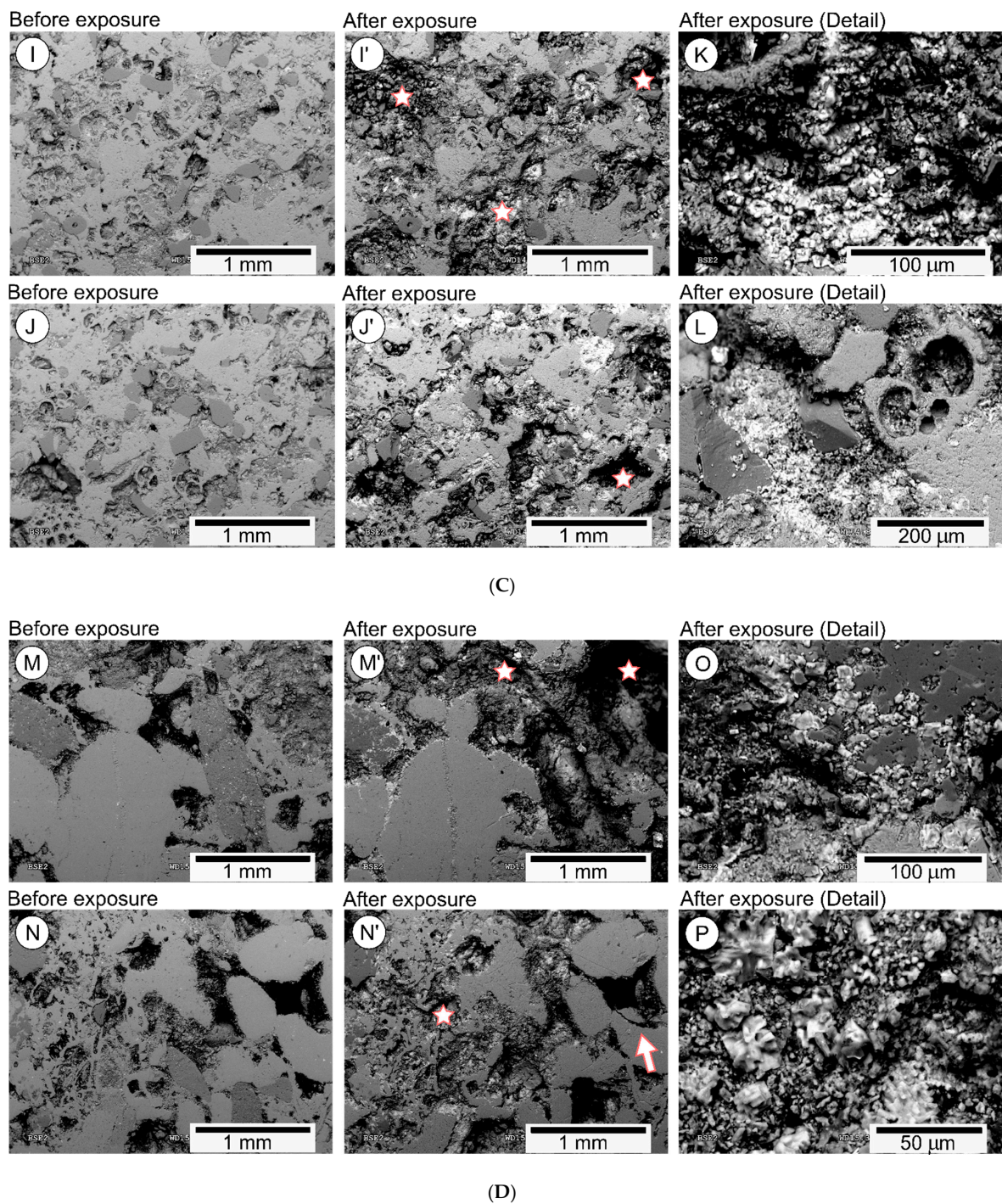


Figure 2. (A) Textural evolution of Mb sample (calcite marble) after direct exposure to marine environment. Images A' and B' correspond to the weathered aspect of A and B. Images C and D are surface details obtained in the red squares of A' and B', respectively. (B) Textural evolution of Ls sample (microcrystalline limestone) after direct exposure to marine environment. Images E' and F' correspond to the weathered aspect of E and F. Arrow in E' shows the apparition of new facies. Image G is a surface detail obtained in the red square of F'. Image H is a surface detail of the weathered surface of Ls sample. (C) Textural evolution of Cf sample (fine-grained calcarenite) after direct exposure to marine environment. Images I' and J' correspond to the weathered aspect of I and J. Stars in I' and J' indicate examples of grain detachment. Images K and L correspond to surface details of the weathered surface of Cf sample. (D) Textural evolution of Cg sample (coarse-grained calcarenite) after direct exposure to marine environment. Images M' and N' correspond to the weathered aspect of M and N. Stars in M' and N' indicate examples of grain detachment. Arrow in N' shows the apparition of new facies. Images O and P correspond to surface details of the weathered surface of Cg sample.

Marble (Mb sample, Figure 2A) shows chemical corrosion of crystal edges and intracrystalline line defects (cleavage planes) (Figure 2A, image D). Martínez-Martínez et al. [16] observed similar dissolution patterns in marbles chemically weathered in brine immersion. Corrosion of samples occurs preferentially on the crystal edges rather than in the interior, due to two main reasons. On the one hand, calcite dissolution occurs by the creation of both shallow and deep pits at the surface [14]. The formation of these pits, especially the deep ones, is likely driven by line defects, contributing to the more intense dissolution of these planes. On the other hand, inter-crystalline cracks constitute moisture flow paths where the contact rock-brine is more prolonged. Evidence of these preferential ways for penetration and evaporation of moisture to and from the inner rock is the presence of saline efflorescences (halite crystals) growing throughout inter-crystalline contacts (Figure 2A, image C).

Microweathering signs on the surface of the massive limestone sample (Ls, Figure 2B) are very similar to those observed on Mb surface but adapted to the microcrystalline texture of Ls rock. The most characteristic decay pattern is the corrosion of crystal edges (Figure 2B, image H). This chemical dissolution is much more intense in calcite than in the dolomite crystals included in the rock mass (dark minerals in Figure 2B, image G). The higher chemical stability of dolomite than calcite has been deeply studied [17,18]. Ls also show calcite veins with high crystal size (up to 0.4 mm) around which cracks are developed during weathering (white arrow in image E', Figure 2B). These cracks result from the coalescence of previous intercrystalline microcracks formed because of widening of intercrystalline contacts.

The two calcarenites (Cf and Cg; Figure 2C,D, respectively) develop similar decay processes. In both cases, grain detachment (examples marked with white stars in photographs I', J', M' and N', Figure 2C,D) and the appearance of efflorescences and subefflorescences (white areas and white crystals in photographs K, L, O and P, Figure 2C,D) are the main weathering signs after one year of direct exposure. Intragranular microcracks also appeared in a few points in Cg (white arrow in image N', Figure 2D).

These results are compatible with the decay patterns and weathering processes observed in the rock blocks of the cultural heritage of the Nueva Tabarca Island. Both porous limestones (Cf and Cg) are extensively used in the local buildings [5]. Salt subefflorescences and grain detachment are the main weathering processes observed in porous limestones (Cf and Cg), resulting in larger decay forms such as differential erosion or honeycomb patterns [5]. After 244 years of exposure, the erosion rates measured in the building stone blocks of the monuments vary between 0.11 and 0.28 mm/year. Despite the submillimetric range of these rates, they are slightly overestimated, taking into account the material loss observed in these rocks under SEM after one year of direct exposure. This fact can be explained because stone decay behaves most often as a non-linear system, and rock weathering degrees do not change proportionally to time [19]. The so-called “catastrophic decay” seems to be particularly common in sandstones [20], but are also found in limestones [21].

All these weathering patterns developed in marine conditions are mainly due to the presence of halite (in its crystalline form or in the brine) in the porous system of the rock. The location of the tested samples on the upper part of the building indicate that salt supply is carried out by sea-spray deposition [1,4]. Once marine aerosol has been deposited on the stone surface, halite is dissolved, and the dissolution penetrates towards the inside of the stone. This process will be more important in those rocks with a higher proportion of micropores (radius lower than 1 μm) because they are the responsible for the moisture adsorption and condensation processes. However, a low penetration depth of the brine inside the rock is expected, leaving a wet layer closer to the stone surface. Then, wind-enhanced evaporation of the saline solution induces the formation of subefflorescence, resulting in granular disintegration [9]. The cyclic repetition of this wet–dry process supposes a continuous supply and flow of salty solution to the rock, favoring the chemical dissolution of soluble minerals (calcite).

Chemical dissolution and halite subefflorescences act mainly as weathering agents (in contraposition to erosion agents), causing the initial weakness of the rock surface, and therefore increasing the efficiency of the subsequent erosive process. Previous studies conclude that, in the semiarid Mediterranean climate, wind-driven rain is revealed as the main erosion process especially due to its torrential character [5].

4.2. Rock Weathering during Thermal Cycles

Figure 3 illustrates the comparison between the linear thermal expansion of the different studied rocks and a pure crystal of halite. The linear thermal expansion coefficient (α_T) of studied rocks range between $0.90 \times 10^{-6} \text{ }^\circ\text{C}^{-1}$ (marble, Mb) and $7.72 \times 10^{-6} \text{ }^\circ\text{C}^{-1}$ (fine-grained sandy calcarenite, Cf). The halite sample shows a noticeable higher thermal expansivity than rocks. This different behaviour during heating was visually checked by means of an Environmental Scanning Electron Microscope (ESEM) (Figure 4). During the test, a pore partially filled with halite crystals was observed during the heating process. As the temperature rises from $3 \text{ }^\circ\text{C}$ to $50 \text{ }^\circ\text{C}$ (image sequence from A to D in Figure 4), the expansion of the crystal length is observed, while the walls of the hosting pore remain unchanging.

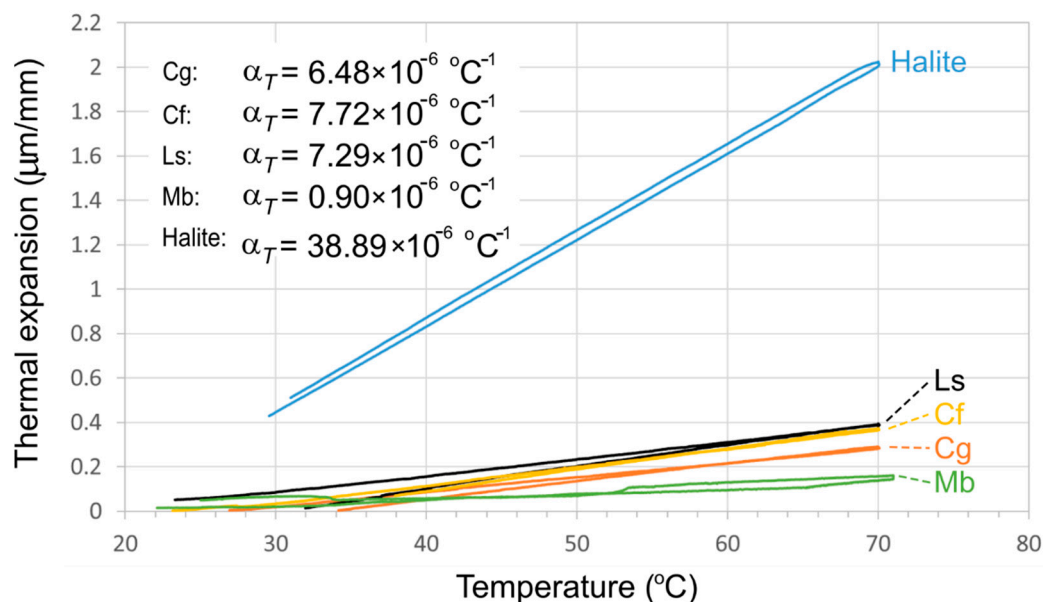


Figure 3. Linear thermal expansion of the different studied rocks and a pure crystal of halite. Cg: coarse-grained calcarenite; Cf: fine-grained calcarenite; Ls: massive limestone; Mb: marble.

Previous studies [11] point out that if the pores of a stone become filled with halite, the mismatch in the coefficient of thermal expansion can be destructive. Given that the thermal stress of halite is roughly equal to the product $E \cdot \Delta\alpha_T \cdot \Delta T$, where E is the Young modulus (35 GPa for halite) and the thermal expansion mismatch between stone and salt ($\Delta\alpha_T$) is $30 \times 10^{-6} \text{ }^\circ\text{C}^{-1}$ approximately, this is about 1 MPa per degree change in temperature. According to this result, the change in temperature from day to night could generate stress exceeding the tensile strength of stone (frequently lower than 10 MPa in this rock types, [22]) This theoretical damage is effective when pores are full of salt, and its effectiveness decreases progressively as the salt filling degree decreases.

Hence, differential thermal expansion can justify (or at least can contribute to justifying) some of the weathering patterns observed during the direct exposure of rocks to the marine semiarid conditions, such as the grain detachment in areas with subefflorescences, as well as the widening and development of microcracks in Ls and Cg (images E' and N' in Figure 2B,D, respectively).

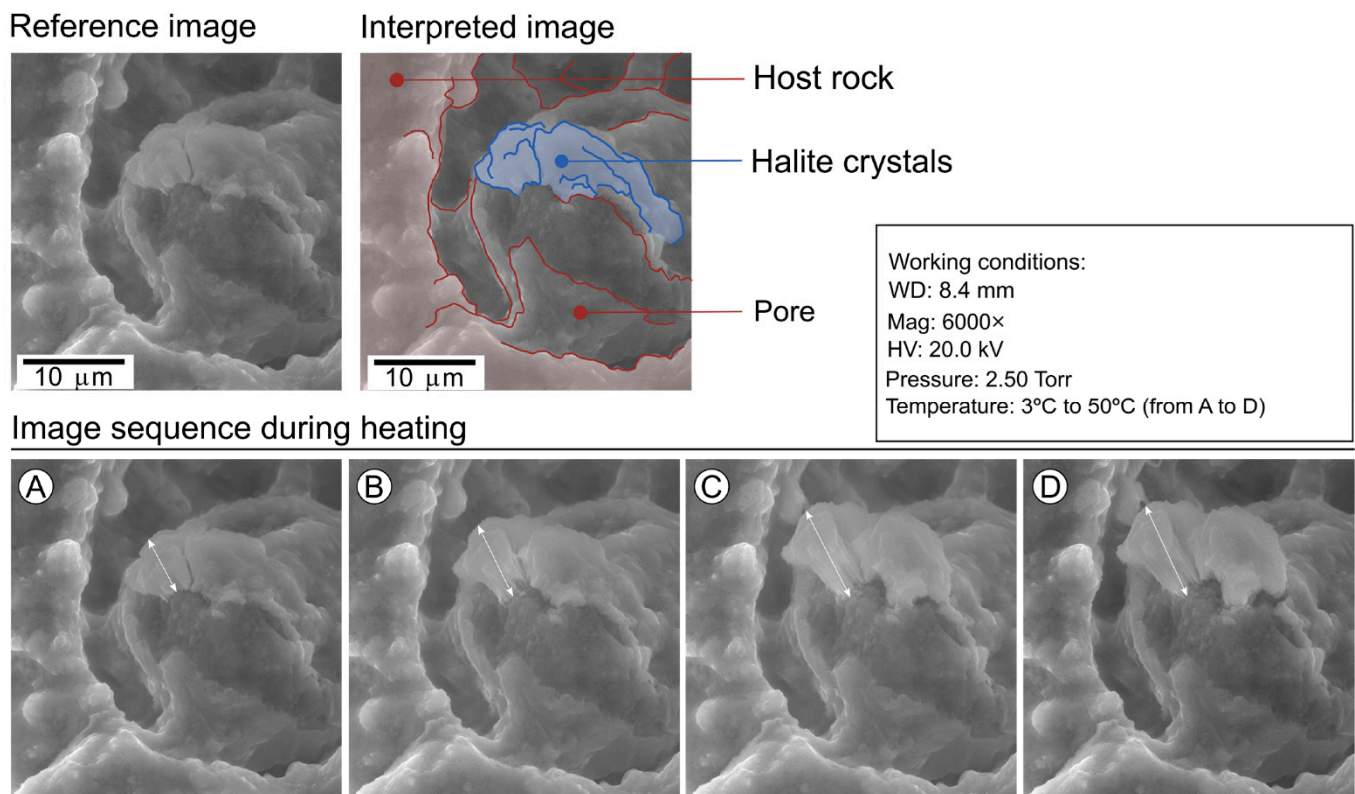


Figure 4. Thermal expansion of halite crystals inside a pore during the heating process. Photographs taken with an Environmental Scanning Electron Microscope (ESEM). Images (A–D) illustrate the evolution of the crystal morphology during the heating process from cold (image A, at 3 °C) to warm conditions (image D, at 50 °C).

The real effectiveness of this weathering process was checked by means of the laboratory simulation in the climatic cabinet. Table 2 shows the weight loss measured in each rock sample after the test. Moreover, mean weight increment per rock variety was also calculated with respect to the initial weight. Results show that thermal expansion of halite present as both efflorescences and subefflorescences in the porous system of rocks is an effective weathering process. It is especially aggressive in porous rocks (weight loss up to 2% after the test), while the weight loss measured in massive varieties (Ls and Mb) is almost zero. In fact, Ls and Mb register a slight increment in the sample weight even after the cleaning process in distilled water. This increment can be explained due to the remaining of small quantities of salts in the tortuous pore network.

Two reasons explain the lower durability of Cf and Cg during the cabinet test. On the one hand, they are much more porous than Mb and Ls (porosity values of Cf and Cg range between 16 and 24%, whilst they are around 1% for Ls and Mb). Porosity controls the amount of salt crystallised inside the rock. The higher the rock capacity to contain salts, the higher the thermal stresses generated during heating processes when pores are completely filled with halite.

On the other hand, the mechanical properties of rocks are a key factor for rock durability due to the fact that strength is the material's resistance to weathering processes. When the tensile strength of a rock is lower than or similar to the thermal stresses generated during thermal dilation of halite inside pores, rock tends to suffer disintegration, detachment and fracturation at the outer layers of the block [11,23]. In this sense, Cf and Cg are softer than Mb and Ls. According to previous works, Cf and Cg compressive strength ranges between 19.69 and 44.22 MPa [5], whilst the mean value for Ls is around 110.10 MPa and 89.41 MPa for Mb [16].

Table 2. Weights measured in each rock sample before and after the thermal cycles in climatic cabinet. Three samples (A, B and C) per rock variety were tested. Mean weight increment (%) per rock variety is also calculated with respect to the initial weight.

Sample	Initial State	After Salt Saturation	After Cabinet Test		
			With Salts	After Salt Removing	
Ls	A	34.1	34.66	34.66	34.11
	Weight (g) B	34.46	34.98	34.98	34.48
	C	24.86	25.29	25.28	24.85
	Mean Weight increment (%)		1.69	1.61	0.02
Cf	A	38.91	41.88	41.01	38.13
	Weight (g) B	44.85	47.68	46.55	43.97
	C	42.69	45.55	44.6	41.89
	Mean Weight increment (%)		6.88	4.55	−1.95
Cg	A	54.03	58.98	57.84	53.15
	Weight (g) B	49.66	54.5	53.58	49.02
	C	50.07	54.89	53.78	49.2
	Mean Weight increment (%)		9.51	7.45	−1.55
Mb	A	48.96	48.98	48.98	48.97
	Weight (g) B	47.51	47.5	47.5	47.5
	C	52.81	52.84	52.84	52.82
	Mean Weight increment (%)		0.02	0.02	0.01

4.3. Rock Weathering during Brine Immersion Test

Figure 5 illustrates the weathered surface of the rocks tested in the brine immersion test. Observations corroborate the preferential chemical corrosion of crystal edges and intra-crystalline line defects, rather than discontinuity-free crystal areas. The solubility of calcite is higher in NaCl solutions than in pure water [24]. Calcite solubility increases about 2% with 1 mmol of dissolved NaCl and about 10% with 10 mmols [25]. At the same time, the presence of sodium chloride in solution also accelerates the dissolution of calcite. Nevertheless, calcite dissolution in basic media (brines) is much less aggressive than in acid solutions, common in meteoric waters in polluted air environments [26].

The resulting weathered textures of Mb and Ls are very similar to those observed after the direct exposure of samples to the marine environment, confirming that the chemical dissolution of calcite minerals acts as an effective weathering agent during rock exposure under marine conditions.

Mineral corrosion modifies the characteristics of the porous system of rocks, increasing in most of the cases the pore connection, and lastly favouring the effectiveness of posterior weathering agents. Figure 6 shows the MIP curves obtained in the fresh and weathered rock samples before and after the brine immersion test, respectively. For all the rocks, the porosity is higher in the weathered samples than in the fresh ones. Even if this porosity increase, in absolute values, is almost negligible (less than 1%) in relative values, it doubles the initial porous content of some of the rocks (Ls, for example). Changes in the pore size distribution are related to: (1) the appearance of new pore families (pore family centred in 0.1 μm in Ls); (2) the increase in volume of some pore families (pore family of 2–10 μm in Mb; or pore family centred in 100 μm in Ls); (3) displacement of the MIP curve to the right (towards bigger pore radii; Cf and Cg curves, for example); (4) displacement of the MIP curve to the left (i.e., towards smaller pore radii; Cf curve).

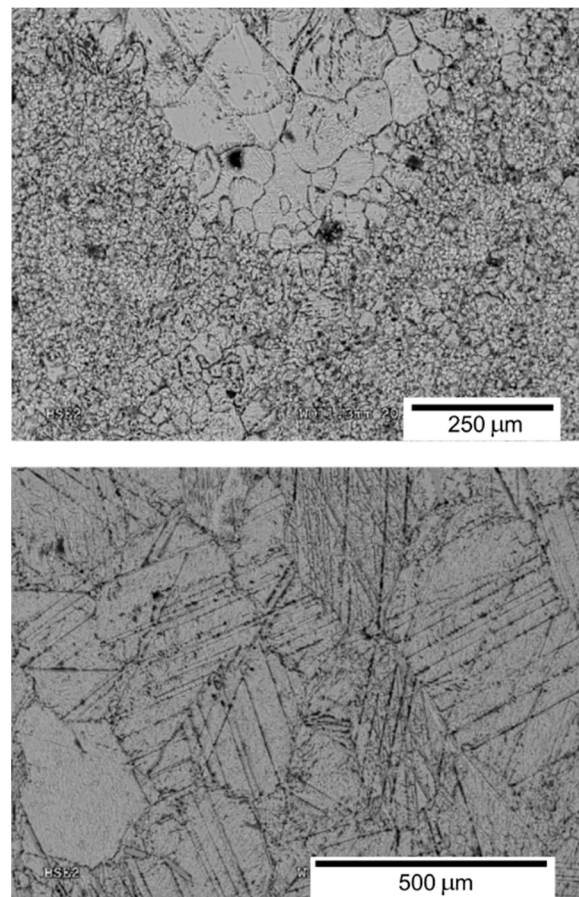


Figure 5. Weathered surface of the rocks tested in the brine immersion test. Photographs taken with a Scanning Electron Microscope.

Angeli et al. [27] analysed the evolution of MIP curves after salt crystallization tests, registering five possible cases for the evolution of the MIP curves after weathering tests. Their conclusions cannot be completely transferred to the discussion of our results due to the fact that they consider the presence of salt crystals in the porous system of rocks. However, the general reasoning used by Angeli et al. explains most of the modifications observed in the MIP curves after the brine immersion test. Firstly, the apparition of new pore families is related to the dissolution of crystal edges, creating a new pore net without connection to the previous porous system. This situation can be only seen in massive crystalline low-porous rocks, such as Ls samples.

Secondly, when the edge dissolution occurs in porous rocks, two situations can be observed. On the one hand, a new micropore net (dissolved inter-crystalline discontinuities) is connected to the previous porous system. In this case, the MIP curve shifts to lower values (displacement to the left) due to the fact that new small entries to the pores are created. This situation could be interpreted as an exaggeration of the ink bottle phenomenon. On the other hand, the dissolved edges constitute the entry to pre-existing chambers. In this case, the dissolution process widens the pore entry, and the MIP curve shifts to bigger values (displacement to the right).

Finally, a global pore wall dissolution (including both pore chamber and entries) can occur in all the porous system of the sample. In this case, an increase in the pore volume is registered in the MIP curve as well as a slight displacement to bigger pore sizes.

According to the above reasoning, chemical dissolution of massive crystalline rocks in a brine immersion tend to create new pore families associated with the dissolution of crystal edges. This new family can either increase the connectivity of the pre-existent porous system (Mb) or create a new pore net without connection with previous pores (Ls).

In the case of porous rocks (Cf and Cg), chemical dissolution causes the widening of pore entries as well as the creation of new micropores that increase the ink bottle character of the porous system.

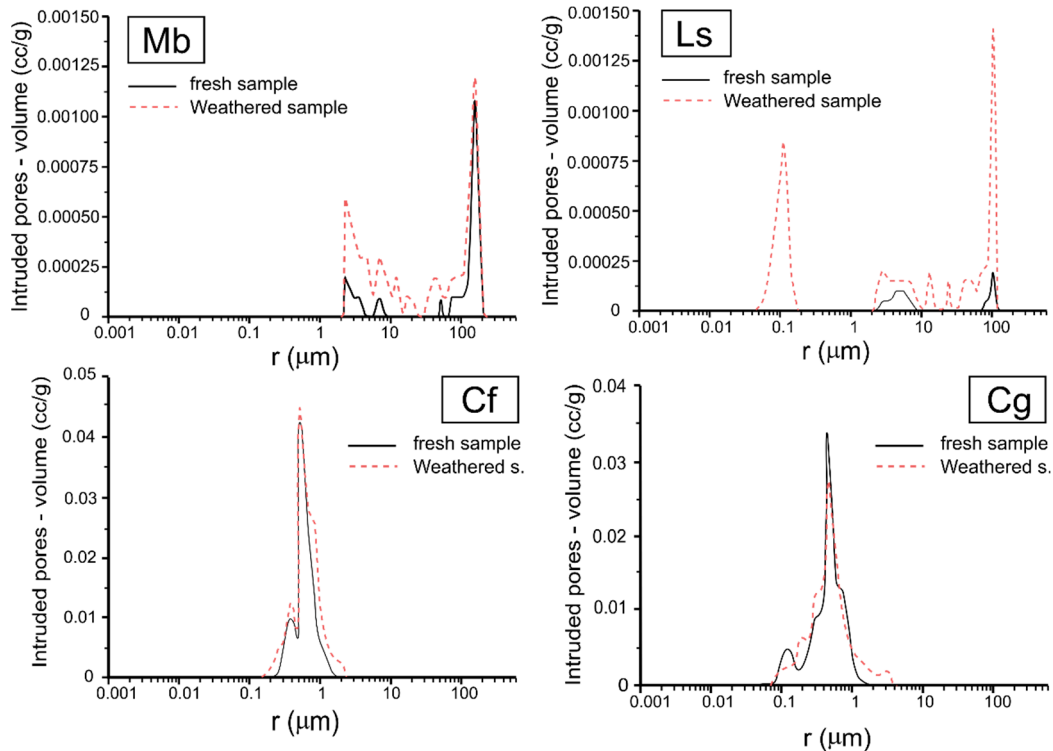


Figure 6. MIP curves obtained in the fresh and weathered rock samples before and after the brine immersion test.

5. Conclusions

The results obtained from this paper demonstrate that mineral dissolution and differential thermal expansion between both halite and hosting rock are active mechanisms of deterioration of calcite-based rocks exposed to marine environments. These conclusions are based on the analysis of the behaviour of four different litypes (a marble, a limestone and two calcarenites) during both environmental direct exposure and laboratory simulations.

Weathered samples after direct exposure do not show noticeable decay signs at mesoscale, but grain detachment, crystal edge corrosion, halite efflorescences and microfissuring were observed under Scanning Electron Microscope. Although all these decay patterns cannot be justified exclusively to the halite–rock interaction due to the fact that other meteorological events act on the rock samples during direct exposure, results obtained from laboratory simulations demonstrate that they can explain most of the rock pathologies.

Laboratory measurements prove that halite crystals have a noticeably higher thermal expansivity than studied rocks. Linear thermal expansion coefficient (α_T) of halite is $38.89 \times 10^{-6} \text{ }^\circ\text{C}^{-1}$, while this coefficient in studied rocks range between $0.90 \times 10^{-6} \text{ }^\circ\text{C}^{-1}$ (marble, Mb) and $7.72 \times 10^{-6} \text{ }^\circ\text{C}^{-1}$ (fine-grained sandy calcarenite, Cf). This difference can justify (or at least can contribute to justifying) some of the weathering patterns observed during the direct exposure of rocks to the marine semiarid conditions, such as the grain detachment in areas with subefflorescences, as well as the widening and development of microcracks.

The real effectiveness of thermal expansivity of halite present as both efflorescences and subefflorescences was demonstrated by means of rock monitoring during thermal cycles in a climatic cabinet. Halite expansivity is especially dangerous in porous rocks, causing weight losses up to 2% after the test.

Weathered samples after the brine immersion test show preferential chemical corrosion of crystal edges and intra-crystalline line defects, similar to those observed after the direct exposure of samples to the marine environment. Mineral corrosion modifies the characteristics of the porous system of rocks, increasing in most of the cases the pore connection and lastly favouring the effectiveness of posterior weathering agents. The comparison of mercury intrusion porosimetry (MIP) curves of fresh and weathered samples corroborates the modification of the pore size distribution, mainly focused on: (1) the appearance of new pore families; (2) an increase in the volume of some pore families; (3) the displacement of the MIP curve to bigger sizes due to the dissolution of pore entries; (4) the displacement of the MIP curve to smaller values, related to the creation of new small entries to the pores.

Author Contributions: Conceptualization, collecting, processing and analyzing the samples, interpreting the results and writing the original draft, J.M.-M.; methodology and interpreting the results, A.A.; interpreting results and finalizing the paper, D.B. All authors have read and agreed to the published version of the manuscript.

Funding: Experimental tests in the cabinet carried out at the University of Oxford were financially supported by the European Commission under the Marie Curie program (FP7-PEOPLE-2012-IEF call, research project “NaturaLime”). This research has been supported by the Spanish Government (MICINN) (PID2020-116896RB-C21 and PID2020-116896RB-C22).

Data Availability Statement: Not applicable.

Conflicts of Interest: The authors declare no conflict of interest.

References

- Cardell, C.; Delalieux, F.; Roumpopoulos, K.; Moropoulou, A.; Auger, F.; Van Grieken, R. Salt-induced decay in calcareous stone monuments and buildings in a marine environment in SW France. *Constr. Build. Mater.* **2003**, *17*, 165–179. [\[CrossRef\]](#)
- Andriani, G.F.; Walsh, N. The effects of wetting and drying, and marine salt crystallization on calcarenite rocks used as building material in historic monuments. *Geol. Soc. Lond. Spec. Publ.* **2007**, *271*, 179–188. [\[CrossRef\]](#)
- Rothert, E.; Eggers, T.; Cassar, J.; Ruedrich, J.; Fitzner, B.; Siegesmund, S. Stone properties and weathering induced by salt crystallization of Maltese Globigerina Limestone. In *Building Stone Decay: From Diagnosis to Conservation*; Prikryl, R., Smith, B.J., Eds.; Geological Society: London, UK, 2015; pp. 189–198.
- Stefanis, N.A.; Theoulakis, P.; Pilinis, C. Dry deposition effect of marine aerosol to the building stone of the medieval city of Rhodes, Greece. *Build. Environ.* **2009**, *44*, 260–270. [\[CrossRef\]](#)
- Martínez-Martínez, J.; Benavente, D.; Jiménez-Gutiérrez, S.; García-del-Cura, M.A.; Ordóñez, S. Stone weathering under Mediterranean semiarid climate in the fortress of Nueva Tabarca island (Spain). *Build. Environ.* **2017**, *121*, 262–276. [\[CrossRef\]](#)
- Colston, B.J.; Watt, D.S.; Munro, H.L. Environmentally-induced stone decay: The cumulative effects of crystallization–hydration cycles on a Lincolnshire oopelsparite limestone. *J. Cult. Herit.* **2001**, *2*, 297–307. [\[CrossRef\]](#)
- Grossi, C.M.; Brimblecombe, P.; Menéndez, B.; Benavente, D.; Harris, I.; Déqué, M. Climatology of salt transitions and implications for stone weathering. *Sci. Total. Environ.* **2011**, *409*, 2577–2585. [\[CrossRef\]](#)
- Goudie, A.S.; Viles, H.A. *Salt Weathering Hazards*; John Wiley: Chichester, UK, 1997; p. 241.
- Rodríguez-Navarro, C.; Doehne, E.; Sebastián, E. Origins of honeycomb weathering: The role of salts and wind. *GSA Bull.* **1999**, *111*, 1250–1255. [\[CrossRef\]](#)
- Doehne, E. Salt weathering: A selective review. In *Natural Stone, Weathering Phenomena, Conservation Strategies and Case Studies*; Siegesmund, S., Weiss, T., Vollbrecht, A., Eds.; Geological Society Special Publication: London, UK, 2002; p. 256.
- Scherer, G.W.; Flatt, R.; Wheeler, G. Materials science research for the conservation of sculpture and monuments. *MRS Bull.* **2001**, *26*, 44–50. [\[CrossRef\]](#)
- Benavente, D.; Sanchez-Moral, S.; Fernández-Cortés, A.; Canaveras, J.C.; Elez, J.; Saiz-Jimenez, C. Salt damage and microclimate in the Postumius Tomb, Roman Necropolis of Carmona, Spain. *Environ. Earth Sci.* **2011**, *63*, 1529–1543. [\[CrossRef\]](#)
- Benavente, D.; Brimblecombe, P.; Grossi, C.M. Thermodynamic calculations for the salt crystallisation damage in porous built heritage using PHREEQC. *Environ. Earth Sci.* **2015**, *74*, 2297–2313. [\[CrossRef\]](#)
- Liang, Y.; Baer, D.R. Anisotropic dissolution at the CaCO₃ {104}–water interface. *Surf. Sci.* **1997**, *373*, 275–287. [\[CrossRef\]](#)
- Benavente, D.; Martínez-Verdú, F.; Bernabéu, A.; Viqueira, V.; Fort, R.; García del Cura, M.A.; Illueca, C.; Ordóñez, S. Influence of Surface roughness on color changes in building stones. *Color Res. Appl.* **2002**, *28*, 343–351. [\[CrossRef\]](#)
- Martínez-Martínez, J.; Benavente, D.; Pérez-Huerta, A.; Cueto, N.; García-del-Cura, M.A. Changes on the Surface properties of foliated marbles at different cutting orientations. *Constr. Build. Mater.* **2019**, *222*, 493–499. [\[CrossRef\]](#)
- Liu, A.; Yuan, D.; Dreybrodt, W. Comparative study of dissolution rate-determining mechanisms of limestone and dolomite. *Environ. Geol.* **2005**, *49*, 274–279. [\[CrossRef\]](#)

18. Luttge, A.; Winkler, U.; Lasaga, A.C. An interferometric study of the dolomite dissolution: A new conceptual model for mineral dissolution. *Geochim. Cosmochim. Acta* **2003**, *67*, 1099–1116. [[CrossRef](#)]
19. Viles, H.A. Can Stone decay be chaotic? In *Stone Decay in the Architectural Environment*; Turkington, A.V., Ed.; Geological Society of America, Special Publication: Boulder, CO, USA, 2005; p. 390.
20. Smith, B.J.; Gomez-Heras, M.; McCabe, S. Understanding the decay of stone-built cultural heritage. *Prog. Phys. Geog.* **2008**, *32*, 361–439. [[CrossRef](#)]
21. Smith, B.J.; Gomez-Heras, M.; Viles, H.A. *Underlying Issues on the Selection Use and Conservation of Building Limestone*; Geological Society, Special Publication: London, UK, 2010; p. 331.
22. Martínez-Martínez, J.; Corbí, H.; Martín-Rojas, I.; Baeza-Carratalá, J.F.; Giannetti, A. Stratigraphy, petrophysical characterization and 3D geological modelling of the historical quarry of Nueva Tabarca island (western Mediterranean): Implications on heritage conservation. *Eng. Geol.* **2017**, *231*, 88–99. [[CrossRef](#)]
23. Benavente, D.; Cueto, N.; Martínez-Martínez, J.; García-del-Cura, M.A.; Cañaveras, J.C. The influence of petrophysical properties on the salt weathering of porous building rocks. *Environ. Earth Sci.* **2007**, *52*, 215–224. [[CrossRef](#)]
24. Millero, F.J.; Milne, P.J.; Thurmond, V.L. The solubility of calcite, strontianite and witherite in NaCl solutions at 25 °C. *Geochim. Cosmochim. Acta* **1984**, *48*, 1141–1143. [[CrossRef](#)]
25. Sanchez-Moral, S.; Soler, V.; Canaveras, J.C.; Sanz-Rubio, E.; Van Grieken, R.; Gysels, K. Inorganic deterioration affecting the Altamira Cave, N Spain: Quantitative approach to wall-corrosion (solutional etching) processes induced by visitors. *Sci. Total. Environ.* **1999**, *244*, 67–84. [[CrossRef](#)]
26. Arvidson, R.S.; Ertan, I.E.; Amonette, J.E.; Luttge, A. Variation in calcite dissolution rates: A fundamental problem? *Geochim. Cosmochim. Acta* **2003**, *67*, 1623–1634. [[CrossRef](#)]
27. Angeli, M.; Benavente, D.; Bigas, J.P.; Menéndez, B.; Hébert, R.; David, C. Modification of the porous network by salt crystallization in experimentally weathered sedimentary stones. *Mater. Struct.* **2008**, *41*, 1091–1108. [[CrossRef](#)]